SAND2022-7610C

Sandia National Laboratories

Exceptional service in the national interest

# NCSD Benchmark Tutorial: Section 2 Evaluation of Experimental Data

David Ames

2022 ANS Annual Meeting
Embedded Topical: NCSD
June 12, 2022
Anaheim, CA

SAND2022-xxxx



U.S. DEPARTMENT OF ENERGY

NNSA

# Purpose of Section 2

The Purpose of Section 2 is to provide an overall evaluation of the experiment

- How good are the data?
- What are the uncertainties?

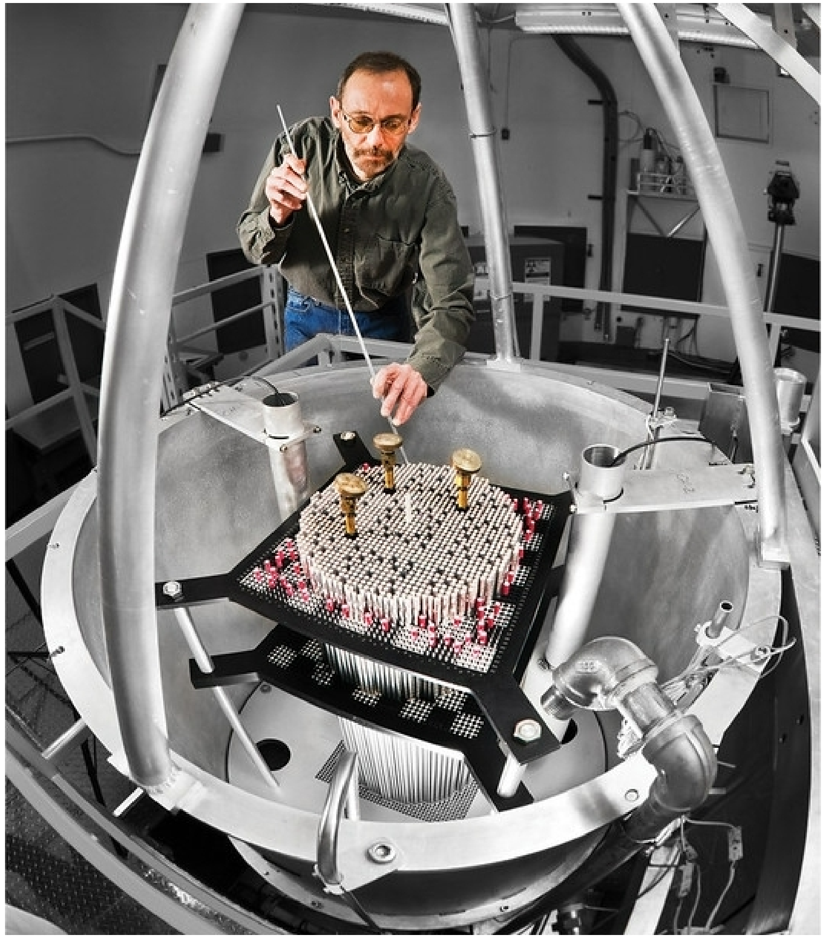

# Document Content and Format Guide for the ICSBEP

- The crit guide provides a good overview and starting point
- The ICSBEP Guide to the Expression of Uncertainties
  - Written to develop a consistency among evaluators in the uncertainty treatment
- New vs historical experiments
  - Similar to discuss on Section 1
- Path can be long and winding
  - Always working on Section 2
  - Typically requires substantial time, effort, and resources.

**Section 2 General Guidelines**

*Evaluation of the experimental data is documented in this section and conclusions are stated and justified. Missing data or weaknesses and inconsistencies in published data are discussed and resolved in appropriate subsections of this section. Uncertainties of $k_{eff}$ due to uncertainties of the experimental data are discussed and quantified. Codes and modeling methods used for calculations of the effects should be specified. Use of data with large uncertainties or data that require questionable assumptions on the part of the evaluator is justified.*

*Besides effects of reported uncertainties, sensitivity of $k_{eff}$ to variation in each parameter whose uncertainty was not reported is calculated or otherwise estimated and provided. If the sensitivity shows that the effect of a rough but reasonable estimate of the uncertainty is negligible, the effect may be evaluated simply as 'negligible.' (The meaning of 'negligible' should be quantified.) Otherwise, a standard uncertainty (i.e., approximate standard deviation[a]) of the parameter is estimated based on whatever information is obtainable, such as typical uncertainty of the parameter at the experimental facility at the time of the experiments, information from the manufacturer of the component or of the measuring device, and personal experience. The basis of the uncertainty estimate should be explained.*

*Differences between code input specifications whose calculated results are subtracted to obtain effects, if not obvious, should be made clear. It is not necessary to use the exact benchmark-model specifications for sensitivity calculations; however, any large discrepancies from the benchmark model should be noted.*

*At the end of Section 2, a summary table showing effects on $k_{eff}$ of the standard uncertainties is presented. It is recommended to also show sensitivities of $k_{eff}$ to the various parameters per unit measure or per 100% and with the sign (+ or -), to preserve in convenient form this outcome of the evaluation. The table concludes with the total combined uncertainty in $k_{eff}$, which is defined as the individual uncertainty effects combined with the measurement uncertainty of the experimentally measured value of $k_{eff}$.*

*If all or some of the configurations are found to be unacceptable for use as benchmark data, this fact is noted in this section, and the reasons are summarized. The evaluation process for the unacceptable configurations is terminated at this point (i.e., unacceptable data are not included in Sections 3, 4, and Appendix A).*

*A decision made by the ICSBEP Working Group that a particular experiment is not acceptable for use as a "Criticality Safety Benchmark Experiment" is not intended to imply that the data, if properly interpreted and applied, cannot be used for validation efforts. In particular, experiments for which the combined uncertainty in the benchmark $k_{eff}$ value exceeds 1% are often judged to be unacceptable. This is especially true when the data are not required to fill gaps in existing data. However, if the large uncertainty is properly taken into account, the data may be used in validation efforts.*

# Section 2 – Content and Format

- Evaluate the data and quantify overall uncertainty through various types of sensitivity analysis
  - Conclusions are state and justified
- Missing data or weakness and inconsistencies in published data are addressed
- Data that require assumptions on part of the evaluator is justified
- The effects of uncertainties are discussed and quantified
  - Every critical experiment has numerous associated uncertainties
    - Contents of the assembly (masses and compositions of constituents)
    - Geometry (dimensions and relative positions)
- If uncertainties are not provided, they must be estimated
- Use of data with large uncertainties is justified
- Summary table showing effects on $k_{eff}$ of the standard uncertainties
- If configurations are found to be unacceptable make note and provide reasoning
  - Unacceptable data are not included in Sections 3, 4 and Appendix A.
- Experiments for which the combined uncertainty in the benchmark $k_{eff}$ exceeds 1% are often judged to be unacceptable.
  - Unacceptable data may still be used in validation efforts if the uncertainty is properly taken into account

# Section 2 (Importance of Uncertainties)

- Benefits
  - Qualifying codes and cross sections used in criticality assessments
  - Improvement of the state of the art of criticality safety
    - Realistic uncertainties from diverse set of experiments provide data needed to uncover weakness in neutron cross section data and calculational methods
    - Path to more accurate criticality safety calculations in the future
- The uncertainty reported in the benchmark evaluation must be as realistic and accurate as possible
  - The analysis must be rigorous, complete, and objective
  - Employ an efficient strategy
    - Little effort needed if a simple estimate shows the uncertainty in a parameter makes a small contribution to the total uncertainty in keff
    - Focus attention and careful consideration on large contributors
- Resist any tendency to overestimate or underestimate uncertainty
  - Unrealistically large total uncertainty – existing biases may be hidden in the uncertainty margins when comparing calculational results and benchmark values
  - Unrealistically low total uncertainty – calculation results may appear erratic or indicate a bias where none exists. This may lead, incorrectly, to modifications of cross sections or lack of confidence in codes or experiments.

# Example - Section 2

- LEU-COMP-THERM-102
  - Pitch Variation Experiments in Water-Moderated Square-Pitched $UO_2$ Fuel Rod Lattices
  - Experiments performed in 2020
  - Available in the 2021 edition of the ICSBEP handbook
  - Similarities to past benchmark evaluations using 7uPCX at Sandia

- Sandia Critical Experiments – Seven Percent Critical Experiments (7uPCX)
  - 6.9 weight perfect $^{235}U$
  - 2175 fuel rods
    - OD ~0.6 cm
    - Fueled length ~48.8 cm
  - Approach-to-critical experiments
    - Number of fuel rods and water height
    - Six critical benchmark evaluations (ICSBEP)

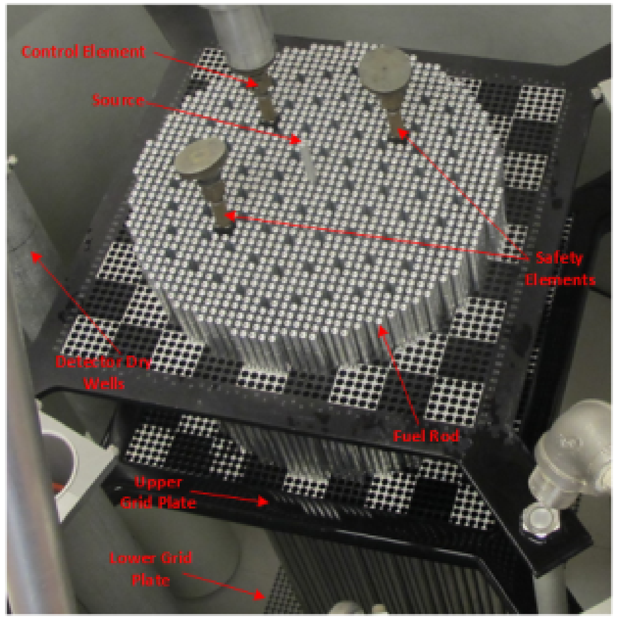


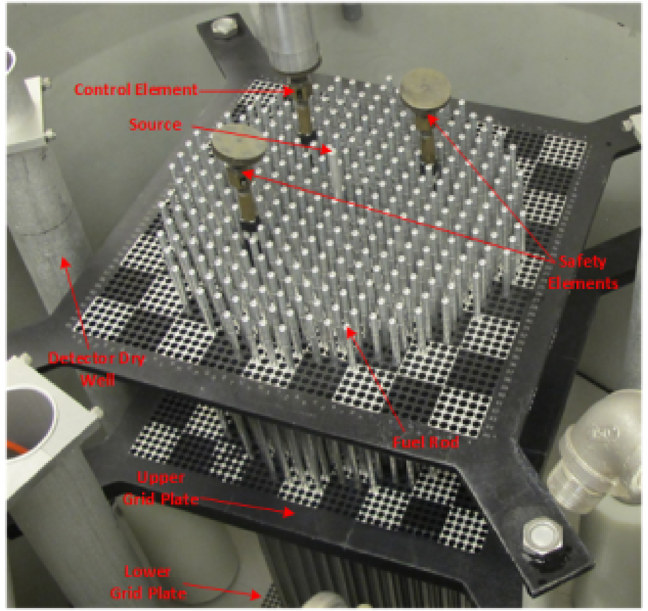

# Example – Section 2 Outline (LEU-COMP-THERM-102)

- 2.0 Evaluation of Experiment Data
- 2.1 Material Data
  - 2.1.1 Fuel Rod $UO_2$ mass
  - 2.1.2 Fuel Impurities
  - 2.1.3 Fuel Rod Cladding
  - 2.1.4 Source Capsule Composition
  - 2.1.5 Fuel Rod Spring Composition
  - 2.1.6 Boron Carbide Composition
- 2.2 Geometric Data
  - 2.2.1 Fuel Rod Pellet Stack Height
  - 2.2.2 Fuel Rod Diameter
  - 2.2.3 Fuel Rod Inner Diameter
  - 2.2.4 Polyethylene Density
  - 2.2.5 Boron Carbide Power Density
- 2.3 Derivation of the Experimental $k_{eff}$
- 2.4 Uncertainty Analyses
  - 2.4.1 Fuel Rod Pitch
  - 2.4.2 Clad Outer Diameter
  - 2.4.3 Clad Inner Diameter
  - 2.4.4 Fuel Outer Diameter
  - 2.4.5 Upper Reflector Thickness
  - 2.4.6 Fuel Rod $UO_2$ Mass
  - 2.4.7 Fuel Rod Pellet Stack Height
  - 2.4.8 Fuel Enrichment
  - 2.4.9 Fuel $^{234}U$ Content
  - 2.4.10 Fuel $^{236}U$ Content
  - 2.4.11 Fuel Stoichiometry
  - 2.4.12 Impurities in the $UO_2$ Fuel
  - 2.4.13 Fuel Clad Composition
  - 2.4.14 Aluminum Grid Plate Composition
  - 2.4.15 Water Composition
  - 2.4.16 Temperature
  - 2.4.17 Uncertainty Values

# Example – Section 2 comparison

- LEU-COMP-THERM-102
  - 2019 - 2021
- 35 pages
- 16 Uncertainties (>1500 of MCNP simulations)
- Reported results of the uncertainty analysis
  - About 0.06 - 0.12 % $\Delta k_{eff}$

- LEU-COMP-THERM-006
  - 1998 (experiments performed 1963 – 1975)
- 2.5 pages
- 7 Uncertainties
- Reported results of the uncertainty analysis
  - About 0.2 % $\Delta k_{eff}$

➢ The process of evaluating and expressing uncertainties has evolved significantly over the lifetime of the ICSBEP
  - Treatment of the uncertainties in earlier evaluations may not meet today’s standards

# Example - Section 2 (LEU-COMP-THERM-102)

- Section 2.0 – Evaluation of Experimental Data

This section provides a confirmation, sometimes after interpretation, of all essential experiment material and geometrical data and provides an analysis of the uncertainties in the experimental configurations. The uncertainties are small for all experiment configurations.

- Section 2.1 – Material Data

**2.1.3 Fuel Rod Cladding –** The clad tubes and end caps for the fuel rods were fabricated from 3003 aluminum. The elemental composition of the 3003 aluminum was not measured. For the work documented here, the composition of the tubes and end caps is assumed to be at the mid-range value where an elemental content is specified as a range and as half of the maximum value where one is given for an element. The composition specification for 3003 aluminum and the composition chosen here are shown in Table 21. The density of the 3003 aluminum was taken as 2.73 g/cm$^3$.[1]

Table 21. Elemental Composition Specification for Aluminum Alloy 3003 and the Composition Used for the Fuel Rod Cladding in the Analyses.

| Element | Specification Composition (Weight %) [a] | Assumed Composition (Weight %) |
|---|---|---|
| Si | 0.6 max | 0.3 |
| Fe | 0.7 max | 0.35 |
| Cu | 0.05 – 0.20 | 0.125 |
| Mn | 1.0 – 1.5 | 1.25 |
| Zn | 0.10 max | 0.05 |
| Other Elements Each | 0.05 max | 0 |
| Other Elements Total | 0.15 max | 0 |
| Al | Remainder | 97.925 |

(a) From ASTM B210-04

[1] From http://matweb.com/search/DataSheet.aspx?MatGUID=fd4a40f87d3f4912925e5e6eab1fbc40 accessed on May 29, 2012. From http://matweb.com search for key word "3003" and choose the "Aluminum 3003-O" option.

# Section 2 vs Section 1 (LEU-COMP-THERM-102)

**1.3.2 Fuel Rod Cladding** – The fabrication drawings for the fuel rods specify the material for the clad tubing and end plugs as aluminum alloy 3003. The composition of the material used was not measured. The specification for the composition of aluminum alloy 3003 is given in Table 12. The density of the cladding material was not measured

Table 12. Chemical Composition Limits of Aluminum Alloy 3003.

| Element | Weight % [a] |
|---|---|
| Si | 0.6 max |
| Fe | 0.7 max |
| Cu | 0.05 – 0.20 |
| Mn | 1.0 – 1.5 |
| Zn | 0.10 max |
| Other Elements Each | 0.05 max |
| Other Elements Total | 0.15 max |
| Al | Remainder |

(a) From ASTM B210-04

**2.1.3 Fuel Rod Cladding –** The clad tubes and end caps for the fuel rods were fabricated from 3003 aluminum. The elemental composition of the 3003 aluminum was not measured. For the work documented here, the composition of the tubes and end caps is assumed to be at the mid-range value where an elemental content is specified as a range and as half of the maximum value where one is given for an element. The composition specification for 3003 aluminum and the composition chosen here are shown in Table 21. The density of the 3003 aluminum was taken as 2.73 g/cm$^3$.[1]

Table 21. Elemental Composition Specification for Aluminum Alloy 3003 and the Composition Used for the Fuel Rod Cladding in the Analyses.

| Element | Specification Composition (Weight %) [a] | Assumed Composition (Weight %) |
|---|---|---|
| Si | 0.6 max | 0.3 |
| Fe | 0.7 max | 0.35 |
| Cu | 0.05 – 0.20 | 0.125 |
| Mn | 1.0 – 1.5 | 1.25 |
| Zn | 0.10 max | 0.05 |
| Other Elements Each | 0.05 max | 0 |
| Other Elements Total | 0.15 max | 0 |
| Al | Remainder | 97.925 |

(a) From ASTM B210-04

# Example - Section 2 (LEU-COMP-THERM-102)

- Section 2.1 – Material Data

**2.1.2 Fuel Impurities** – The fuel pellets were fresh $UO_2$ with measured enrichment and impurity content for ten randomly-chosen fuel pellets. Twelve impurity elements were measured above the detection limit in at least five of the measurements. The measured impurity content and standard deviation of the ten measurements is shown in Table 20. The standard deviations shown for three of the listed elements are larger than the average mass fraction for three impurities – Ag, B, and Cd. This is because each of these species had one measurement that was much higher than the others. Also shown in the table are the thermal absorption cross section for each impurity species and the fraction of the impurity thermal macroscopic absorption cross section contributed by each species. The uncertainty in the impurity macroscopic cross section is dominated by the contribution from boron which is in turn dominated by the fact that one of the measurements is an outlier compared to the rest of the measurements.

Table 20. Fuel Impurity Analysis.

| Species | Mass Fraction[(a)] | Standard Deviation[(b)] | Thermal Absorption Cross Section[(c)] (barns) | Fractional Macroscopic Absorption Cross Section[(d)] | Fractional Contribution to the Macroscopic Absorption Cross Section Uncertainty[(e)] |
|---|---|---|---|---|---|
| Ag | 1.61E-07 | 2.19E-07 | 63 | 0.0022 | 0.0037 |
| B | 4.17E-07 | 4.73E-07 | 760 | 0.6744 | 0.9789 |
| Cd | 2.25E-07 | 3.98E-07 | 2520 | 0.1160 | 0.1928 |
| Co | 2.06E-07 | 5.67E-08 | 37.2 | 0.0030 | 0.0011 |
| Cr | 2.11E-05 | 1.06E-05 | 3.1 | 0.0289 | 0.0190 |
| Cu | 2.19E-06 | 1.59E-06 | 3.8 | 0.0030 | 0.0029 |
| Fe | 9.31E-05 | 4.31E-05 | 2.56 | 0.0982 | 0.0594 |
| Mn | 2.52E-06 | 1.04E-06 | 13.3 | 0.0140 | 0.0076 |
| Mo | 1.93E-06 | 1.85E-06 | 2.5 | 0.0012 | 0.0014 |
| Ni | 3.32E-05 | 1.13E-05 | 4.5 | 0.0586 | 0.0261 |
| V | 1.22E-07 | 2.33E-08 | 5.0 | 0.0003 | 6.9E-05 |
| W | 1.07E-07 | 1.14E-08 | 18.2 | 0.0002 | 3.4E-05 |
| Sum | 1.55E-04[(f)] | – | – | 1.0000[(f)] | 1.0000[(g)] |

(a) The average of the reported impurity mass fractions that were above the detection limit.
(b) The standard deviation of the reported impurity mass fractions that were above the detection limit.
(c) Thermal neutron (2200 m/s) absorption cross section from E. M. Baum, et al., Nuclides and Isotopes Sixteenth Edition, KAPL, Inc., 2002.
(d) The impurity macroscopic absorption cross section is the sum of the [product of the species atom density and the species absorption cross section] having a value of 0.00024 $cm^{-1}$.
(e) The uncertainty in the impurity macroscopic absorption cross section is the sum in quadrature of the [product of the uncertainty in the species atom density and the species absorption cross section] and has a value of 0.00021 $cm^{-1}$.
(f) Arithmetic sum.
(g) Sum in quadrature.

# Section 2 vs Section 1 (LEU-COMP-THERM-102)

### 1.3.1 $UO_2$ Fuel

Metallic impurities were also obtained during the ICP-MS measurements of the ten fuel pellets. The results of the impurity measurements are shown in Table 11.

Table 11. Results of the Fuel Impurity Measurements.

| Element | Average[(a)] (g/g) | Standard Deviation[(a)] (g/g) | Maximum[(b)] (g/g) | Minimum[(c)] (g/g) | Reported Detection Limit[(d)] (g/g) | Measurements Above Detection Limit |
|---|---|---|---|---|---|---|
| Ag | 1.61E-07 | 2.19E-07 | 6.67E-07 | 2.24E-08 | 2.24E-08 | 9 |
| B | 4.17E-07 | 4.73E-07 | 1.56E-06 | 2.24E-08 | 2.24E-08 | 9 |
| Cd | 2.25E-07 | 3.98E-07 | 9.36E-07 | 2.21E-08 | 2.27E-08 | 5 |
| Co | 2.06E-07 | 5.67E-08 | 3.13E-07 | 1.27E-07 | - | 10 |
| Cr | 2.11E-05 | 1.06E-05 | 4.03E-05 | 1.31E-05 | - | 10 |
| Cu | 2.19E-06 | 1.59E-06 | 4.95E-06 | 2.26E-07 | 2.26E-07 | 9 |
| Fe | 9.31E-05 | 4.31E-05 | 1.79E-04 | 5.27E-05 | - | 10 |
| Mn | 2.52E-06 | 1.04E-06 | 4.51E-06 | 1.50E-06 | - | 10 |
| Mo | 1.93E-06 | 1.85E-06 | 5.19E-06 | 6.34E-07 | - | 10 |
| Ni | 3.32E-05 | 1.13E-05 | 5.73E-05 | 2.31E-05 | - | 10 |
| V | 1.22E-07 | 2.33E-08 | 1.56E-07 | 9.71E-08 | - | 10 |
| W | 1.07E-07 | 1.14E-08 | 1.23E-07 | 8.53E-08 | - | 10 |
| Sm | 5.31E-08 | - | 5.31E-08 | 2.21E-08 | 2.27E-08 | 1 |
| Dy | - | - | - | - | 2.27E-08 | 0 |
| Eu | - | - | - | - | 2.27E-08 | 0 |
| Gd | - | - | - | - | 2.27E-08 | 0 |

### 2.1.2 Fuel Impurities

Table 20. Fuel Impurity Analysis.

| Species | Mass Fraction[(a)] | Standard Deviation[(b)] | Thermal Absorption Cross Section[(c)] (barns) | Fractional Macroscopic Absorption Cross Section[(d)] | Fractional Contribution to the Macroscopic Absorption Cross Section Uncertainty[(e)] |
|---|---|---|---|---|---|
| Ag | 1.61E-07 | 2.19E-07 | 63 | 0.0022 | 0.0037 |
| B | 4.17E-07 | 4.73E-07 | 760 | 0.6744 | 0.9789 |
| Cd | 2.25E-07 | 3.98E-07 | 2520 | 0.1160 | 0.1928 |
| Co | 2.06E-07 | 5.67E-08 | 37.2 | 0.0030 | 0.0011 |
| Cr | 2.11E-05 | 1.06E-05 | 3.1 | 0.0289 | 0.0190 |
| Cu | 2.19E-06 | 1.59E-06 | 3.8 | 0.0030 | 0.0029 |
| Fe | 9.31E-05 | 4.31E-05 | 2.56 | 0.0982 | 0.0594 |
| Mn | 2.52E-06 | 1.04E-06 | 13.3 | 0.0140 | 0.0076 |
| Mo | 1.93E-06 | 1.85E-06 | 2.5 | 0.0012 | 0.0014 |
| Ni | 3.32E-05 | 1.13E-05 | 4.5 | 0.0586 | 0.0261 |
| V | 1.22E-07 | 2.33E-08 | 5.0 | 0.0003 | 6.9E-05 |
| W | 1.07E-07 | 1.14E-08 | 18.2 | 0.0002 | 3.4E-05 |
| Sum | 1.55E-04[(f)] | – | – | 1.0000[(f)] | 1.0000[(g)] |

(a) The average of the reported impurity mass fractions that were above the detection limit.
(b) The standard deviation of the reported impurity mass fractions that were above the detection limit.
(c) Thermal neutron (2200 m/s) absorption cross section from E. M. Baum, et al., Nuclides and Isotopes Sixteenth Edition, KAPL, Inc., 2002.
(d) The impurity macroscopic absorption cross section is the sum of the [product of the species atom density and the species absorption cross section] having a value of 0.00024 $cm^{-1}$.
(e) The uncertainty in the impurity macroscopic absorption cross section is the sum in quadrature of the [product of the uncertainty in the species atom density and the species absorption cross section] and has a value of 0.00021 $cm^{-1}$.
(f) Arithmetic sum.
(g) Sum in quadrature.

# Example - Section 2 (LEU-COMP-THERM-102)

- Section 2.2 – Geometric Data

**2.2.2 Fuel Rod Diameter –** The outer diameter of each fuel rod was measured. The average for the population of 2194 fuel rods available for the experiments (5 fuel rods removed from service) was 0.634948 cm with a standard deviation of 0.000218 cm. The average outer diameter of the fuel rods for the specific fuel rods included in the benchmark experiment configurations is listed in Table 26.

Table 26. Average Fuel Rod Outer Diameter in Each Configuration.

| Case | Number of Fuel Rods | Average Fuel Rod Outer Diameter (cm) | |
|---|---|---|---|
| | | Value | Standard Deviation |
| 1 | 1461 | 0.634980 | 0.000216 |
| 2 | 1456 | 0.634981 | 0.000216 |
| 3 | 1424 | 0.634983 | 0.000216 |
| 4 | 1360 | 0.634985 | 0.000215 |
| 5 | 1284 | 0.634989 | 0.000216 |
| 6 | 1204 | 0.634991 | 0.000217 |
| 7 | 1057 | 0.634990 | 0.000207 |
| 8 | 1056 | 0.634990 | 0.000207 |
| 9 | 1028 | 0.634989 | 0.000208 |
| 10 | 980 | 0.634987 | 0.000207 |
| 11 | 928 | 0.634988 | 0.000209 |
| 12 | 465 | 0.634989 | 0.000205 |
| 13 | 464 | 0.634988 | 0.000205 |
| 14 | 456 | 0.634988 | 0.000205 |
| 15 | 444 | 0.634988 | 0.000207 |
| 16 | 413 | 0.634985 | 0.000199 |
| 17 | 412 | 0.634984 | 0.000199 |
| 18 | 408 | 0.634981 | 0.000200 |
| 19 | 398 | 0.634981 | 0.000202 |
| 20 | 338 | 0.634996 | 0.000217 |
| 21 | 339 | 0.634994 | 0.000218 |
| 22 | 345 | 0.634995 | 0.000215 |
| 23 | 347 | 0.634997 | 0.000217 |
| 24 | 346 | 0.634994 | 0.000216 |
| 25 | 349 | 0.634993 | 0.000217 |
| 26 | 361 | 0.634995 | 0.000216 |
| 27 | 367 | 0.634991 | 0.000217 |

# Example - Section 2 (LEU-COMP-THERM-102)

- Section 2.3 – Derivation of the Experiment $k_{eff}$

The approach-to-critical experiments reported here were done with the number of fuel rods in the critical assembly as the approach variable. Once the critical configuration had been measured, the high-multiplication part of the approach-to-critical was repeated using closely-spaced fuel arrays. For square pitched arrays, symmetrical configurations occur at four or eight fuel rod intervals. During the experiments, measurements were made with arrays that were either these symmetrical configurations or fell at an even number of rod intervals between symmetrical configurations.

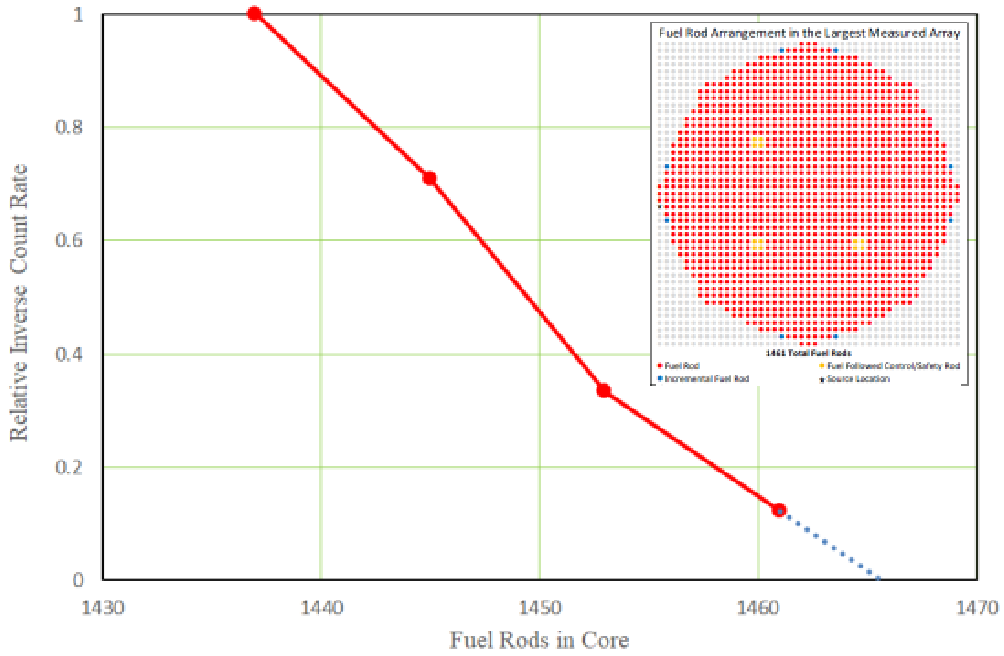


Figure 48. Measured Relative Inverse Count Rate for Case 1.

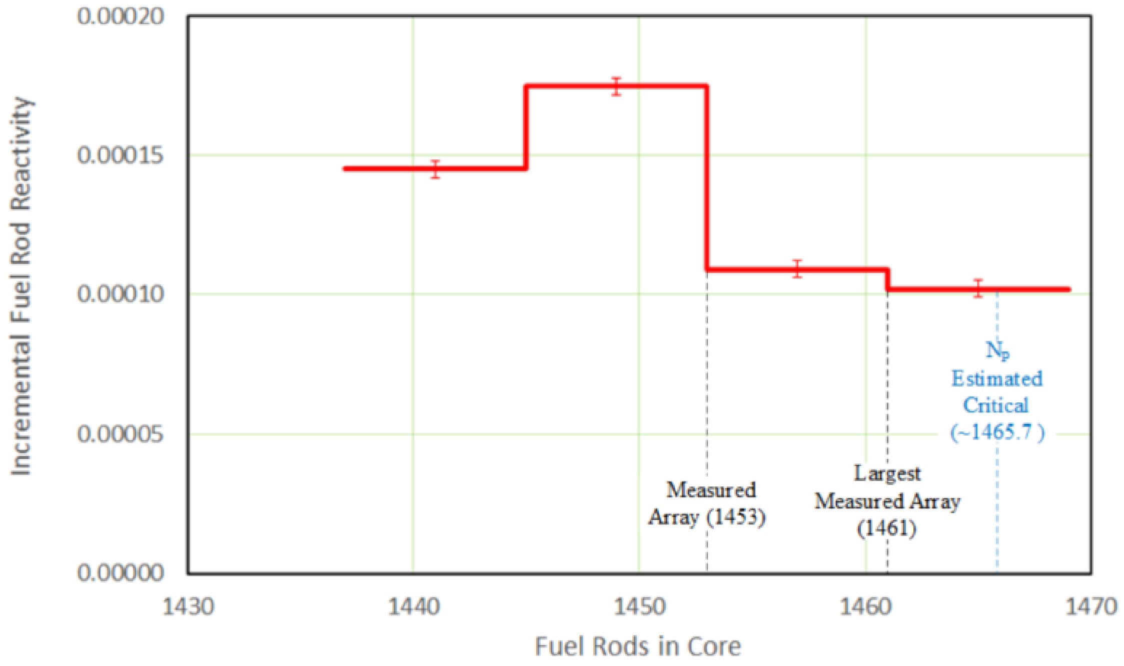


Figure 49. Calculated Fuel Rod Worth Near Delayed Critical for Case 1.

# Example - Section 2 (LEU-COMP-THERM-102)

- Section 2.3 – Derivation of the Experiment $k_{eff}$

In each core configuration, the measured arrays were analyzed using MCNP6.2 with continuous-energy ENDF/B-VII.1 cross sections. The calculated incremental reactivity worth Δρ of each fuel rod in a symmetrical fuel increment (described above) of ΔN rods was determined from

$$\Delta\rho = \frac{k_1 - k_0}{k_1 k_0 \Delta N}$$

The reactivity difference $\rho_{1461}$ between the array with 1461 rods and the projected critical array at $N_p$ is given by

$$\rho_{1461} = (1461 - N_P)\Delta\rho.$$

Knowing that the $k_{eff}$ for an array with $N_p$ rods is 1, the $k_{eff}$ for the array with 1461 fuel rods, $k_{1461}$, is obtained by inverting the definition of the reactivity as

$$k_{1461} = \frac{1}{(1-\rho_{1461})} = \frac{1}{1-(1461-N_P)\Delta\rho}.$$

Table 28. $k_{eff}$ Values Derived from the Projections to Delayed Critical.

| Case | Largest Measured Array (a) | | | Smaller Measured Array | | |
|---|---|---|---|---|---|---|
| | Fuel Rods | $k_{eff}$ | Uncertainty (b) | Fuel Rods | $k_{eff}$ | Uncertainty (b) |
| 1 | 1461 | 0.99949 | 0.00014 | 1453 | 0.99862 | 0.00015 |
| 2 | 1456 | 0.99935 | 0.00014 | 1452 | 0.99891 | 0.00015 |
| 3 | 1424 | 0.99923 | 0.00017 | 1416 | 0.99820 | 0.00017 |
| 4 | 1360 | 0.99941 | 0.00017 | 1356 | 0.99885 | 0.00017 |
| 5 | 1284 | 0.99965 | 0.00015 | 1280 | 0.99912 | 0.00016 |
| 6 | 1204 | 0.99926 | 0.00015 | 1200 | 0.99872 | 0.00015 |
| 7 | 1057 | 0.99900 | 0.00020 | 1053 | 0.99814 | 0.00020 |
| 8 | 1056 | 0.99936 | 0.00020 | 1052 | 0.99851 | 0.00020 |
| 9 | 1028 | 0.99918 | 0.00017 | 1024 | 0.99846 | 0.00017 |
| 10 | 980 | 0.99856 | 0.00019 | 972 | 0.99690 | 0.00019 |
| 11 | 928 | 0.99955 | 0.00019 | 924 | 0.99863 | 0.00019 |
| 12 | 465 | 0.99959 | 0.00022 | 463 | 0.99855 | 0.00022 |
| 13 | 464 | 0.99974 | 0.00022 | 462 | 0.99870 | 0.00022 |
| 14 | 456 | 0.99952 | 0.00021 | 454 | 0.99848 | 0.00021 |
| 15 | 444 | 0.99934 | 0.00021 | 442 | 0.99831 | 0.00021 |
| 16 | 413 | 0.99910 | 0.00020 | 411 | 0.99800 | 0.00020 |
| 17 | 412 | 0.99892 | 0.00021 | 410 | 0.99782 | 0.00020 |
| 18 | 408 | 0.99925 | 0.00020 | 406 | 0.99815 | 0.00020 |
| 19 | 398 | 0.99861 | 0.00020 | 396 | 0.99748 | 0.00020 |
| 20 | 338 | 0.99959 | 0.00019 | 336 | 0.99837 | 0.00018 |
| 21 | 339 | 0.99922 | 0.00019 | 337 | 0.99798 | 0.00019 |
| 22 | 345 | 0.99882 | 0.00018 | 343 | 0.99765 | 0.00018 |
| 23 | 347 | 0.99954 | 0.00017 | 345 | 0.99843 | 0.00017 |
| 24 | 346 | 0.99907 | 0.00018 | 344 | 0.99793 | 0.00018 |
| 25 | 349 | 0.99949 | 0.00018 | 345 | 0.99718 | 0.00018 |
| 26 | 361 | 0.99969 | 0.00018 | 357 | 0.99752 | 0.00017 |
| 27 | 367 | 0.99951 | 0.00016 | 365 | 0.99856 | 0.00016 |

(a) Many of the larger measured arrays fell between the symmetrical arrays listed in Table 36. This occurred for the larger measured arrays in Cases 2, 4, 5, 6, 7, 9, 11–18, 20–24, and 27.

(b) The uncertainties account for the stochastic nature of the radiation process, the uncertainty in the reproducibility of the projections to delayed critical, and the uncertainties in the calculation of the incremental fuel rod reactivity worth.

# Example - Section 2 (LEU-COMP-THERM-102)

- Section 2.4 – Uncertainty Analyses

Performed using MCNP with ENDF/B-VII.1 cross section set.

- Geometry and mass – direct perturbation analyses
  1. Fuel Rod Pitch
  2. Clad Outer Diameter
  3. Clad Inner Diameter
  4. Fuel Outer Diameter
  5. Upper Reflector Thickness
  6. Fuel Rod $UO_2$ Mass
  7. Fuel Rod Pellet Stack Height
- Nuclear Data – adjoint weighting perturbation (KSEN)
  8. Fuel Enrichment
  9. $^{234}U$ Content
  10. $^{236}U$ Content
  11. Fuel Stoichiometry
  12. Impurities in the Fuel
  13. Clad Composition
  14. Grid Plate Composition
  15. Water Composition
- Moderator, reflector, and fuel temperature
  16. Temperature (includes density, thermal expansion, and appropriate nuclear data sets)

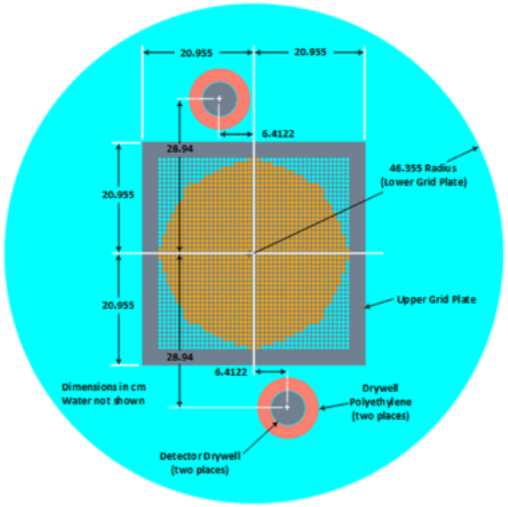


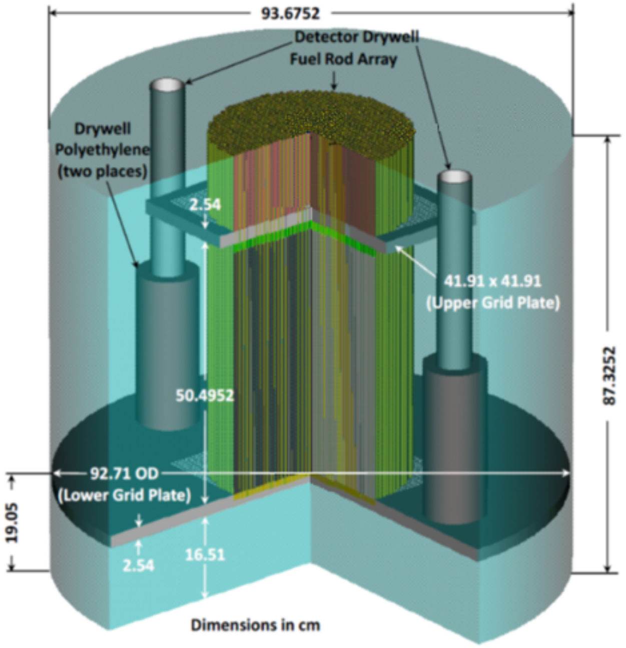


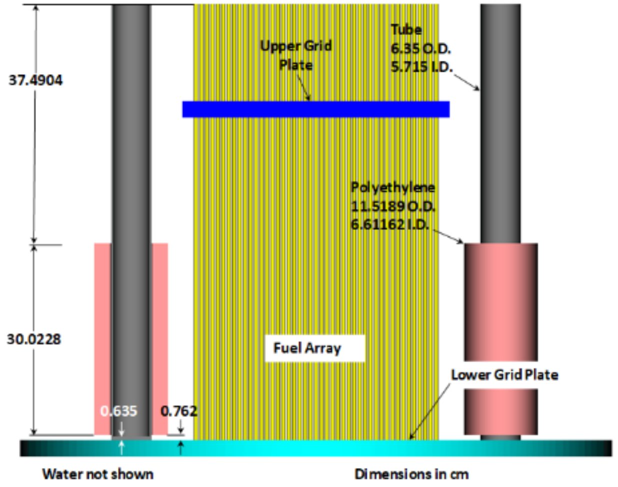

# Example - Section 2 (LEU-COMP-THERM-102)

- Section 2.4 – Uncertainty Analyses

**2.4.1 Fuel Rod Pitch –** The uncertainty in the fuel rod pitch contributes to the uncertainty in the amount of water moderator in the core. This uncertainty is related to the uncertainty in the placement of the holes in the grid plates during fabrication, to the width of the nominal gap between the outside of the fuel rods and the inside of the grid plate holes, to the uncertainty in the diameter of the holes in the grid plates, to the uncertainty in the outside diameter of the fuel rods, and to the number of rows of fuel rods in the core.

Arrays with fuel rod pitch up to 0.01 cm on either side of the nominal value in 0.005 cm increments were analyzed to obtain the effect of pitch on $k_{eff}$. The results were used in a least-squares linear fit to determine the sensitivity of the experiment to the fuel rod pitch. The sensitivity was combined with the pitch uncertainty to obtain the uncertainty in the benchmark experiment $k_{eff}$. The results of these calculations are shown in Table 29.

- Multiple contributors to the uncertainty
  - Placement of the holes in the grid plate
  - Width of the gap between the outside of the fuels rods and inside of the grid plate holes
  - Diameter of the holes in the grid plate
  - Outside diameter of the fuel rods
  - Number of rows of fuel rods in the core
- Direct perturbation analysis
  - Sensitivity and uncertainty value combined to determine $\Delta k_{eff}$

# Example - Section 2 (LEU-COMP-THERM-102)

- Section 2.4 – Uncertainty Analyses

Multiple contributors to the uncertainty

- Placement of the holes in the grid plate
- Width of the gap between the outside of the fuels rods and inside of the grid plate holes
- Diameter of the holes in the grid plate
- Outside diameter of the fuel rods
- Number of row of fuel rods in the core

Direct perturbation analysis

Table 29. Results of the Analysis of the Pitch Uncertainty.

| Case | Fuel Rods on Chord | Uncertainty Value (cm) | Sensitivity ($cm^{-1}$) | | $\Delta k_{eff}$ | |
|---|---|---|---|---|---|---|
| | | | Value | Uncertainty | Value | Uncertainty |
| 1 | 45 | 0.0005589 | 1.3144 | 0.0014 | 0.000735 | 0.000001 |
| 2 | 45 | 0.0005589 | 1.3178 | 0.0014 | 0.000737 | 0.000001 |
| 3 | 43 | 0.0005856 | 1.3032 | 0.0014 | 0.000763 | 0.000001 |
| 4 | 43 | 0.0005856 | 1.2688 | 0.0014 | 0.000743 | 0.000001 |
| 5 | 41 | 0.0006148 | 1.2364 | 0.0014 | 0.000760 | 0.000001 |
| 6 | 41 | 0.0006148 | 1.1958 | 0.0014 | 0.000735 | 0.000001 |
| 7 | 37 | 0.0006832 | 1.0690 | 0.0014 | 0.000730 | 0.000001 |
| 8 | 37 | 0.0006832 | 1.0630 | 0.0014 | 0.000726 | 0.000001 |
| 9 | 37 | 0.0007233 | 1.0444 | 0.0014 | 0.000713 | 0.000001 |
| 10 | 35 | 0.0007233 | 1.0138 | 0.0014 | 0.000733 | 0.000001 |
| 11 | 35 | 0.0007233 | 0.9792 | 0.0014 | 0.000708 | 0.000001 |
| 12 | 25 | 0.0010247 | 0.5736 | 0.0014 | 0.000588 | 0.000001 |
| 13 | 25 | 0.0010247 | 0.5762 | 0.0014 | 0.000590 | 0.000001 |
| 14 | 25 | 0.0010247 | 0.5424 | 0.0014 | 0.000556 | 0.000001 |
| 15 | 25 | 0.0010247 | 0.5182 | 0.0013 | 0.000531 | 0.000001 |
| 16 | 23 | 0.0011179 | 0.4308 | 0.0014 | 0.000482 | 0.000002 |
| 17 | 23 | 0.0011179 | 0.4192 | 0.0014 | 0.000469 | 0.000002 |
| 18 | 23 | 0.0011179 | 0.3942 | 0.0014 | 0.000441 | 0.000002 |
| 19 | 23 | 0.0011179 | 0.3704 | 0.0013 | 0.000414 | 0.000002 |
| 20 | 21 | 0.0012297 | -0.0452 | 0.0011 | -0.000056 | 0.000001 |
| 21 | 21 | 0.0012297 | -0.0538 | 0.0011 | -0.000066 | 0.000001 |
| 22 | 21 | 0.0012297 | -0.0986 | 0.0011 | -0.000121 | 0.000001 |
| 23 | 23 | 0.0011179 | -0.1448 | 0.0011 | -0.000162 | 0.000001 |
| 24 | 21 | 0.0012297 | -0.1752 | 0.0011 | -0.000215 | 0.000001 |
| 25 | 21 | 0.0012297 | -0.1770 | 0.0011 | -0.000218 | 0.000001 |
| 26 | 23 | 0.0011179 | -0.2266 | 0.0011 | -0.000253 | 0.000001 |
| 27 | 23 | 0.0011179 | -0.2614 | 0.0011 | -0.000292 | 0.000001 |

# Example - Section 2 (LEU-COMP-THERM-102)

- Section 2.4 – Uncertainty Analyses

**2.4.12 Impurities in the $UO_2$ Fuel** – The impurities in the fuel fell into two classes – those for which a definite value was measured and those that were determined to be less than the detection limit for the analysis system. For the impurities that were detected, an uncertainty at the one-standard-deviation level of 50 % of the detected value was assumed. For the impurities that were below a detection limit, the uncertainty at one standard deviation was assumed to be equal to the detection limit.

Under the assumption that the fuel mass and volume are held constant, the sensitivity of the system $k_{eff}$ $S_C$ due to the uncertainty in any given impurity can be obtained from

$$S_C = \frac{S_I}{N_I} - \frac{A_I S_{UO2}}{M_{OU2} N_{UO2}}$$

where the symbols $S$, $N$, and $A$ indicate the same quantities as above; the subscript I refers to the impurity species and the subscript $UO2$ refers to the $UO_2$ in the fuel; and $M_{UO2}$ is the molecular weight of the $UO_2$ in the fuel. The uncertainty in $S_C$ is obtained by propagating the uncertainties in $S_I$ and $S_{UO2}$ through the definition of $S_C$. Table 40 lists the uncertainty in the atom density of each fuel impurity, the sensitivity of the system $k_{eff}$ to the atom density uncertainties, and the $k_{eff}$ uncertainty that results from the uncertainty in each impurity for Case 1. The $k_{eff}$ uncertainties for the individual impurities are summed in quadrature to obtain the overall contribution to the uncertainty in the system $k_{eff}$.

# Section 2 (LEU-COMP-THERM-102)

- Section 2.4 – Uncertainty Analyses

### 2.4.12 Impurities in the $UO_2$ Fuel

Table 40. Atom Density Uncertainty and $k_{eff}$ Sensitivity for the Fuel Impurities for Case 1.

| Impurity | Uncertainty ($b^{-1}$ $cm^{-1}$) | Sensitivity (b cm) | | $\Delta k_{eff}$ |
|---|---|---|---|---|
| | | Value | Unc. | |
| Ag | 4.616E-09 | -2.523E+02 | 1.312E+01 | -0.000001 |
| B | 1.193E-07 | -5.909E+02 | 2.239E+00 | -0.000070 |
| Cd | 6.190E-09 | -3.336E+03 | 1.765E+01 | -0.000021 |
| Co | 1.081E-08 | -4.905E+01 | 1.846E+01 | -0.000001 |
| Cr | 1.255E-06 | -1.767E+00 | 7.309E-01 | -0.000002 |
| Cu | 1.066E-07 | -4.512E-01 | 3.265E+00 | 0.000000 |
| Fe | 5.156E-06 | -1.642E+00 | 4.306E-01 | -0.000008 |
| Mn | 1.419E-07 | -8.444E+00 | 5.289E+00 | -0.000001 |
| Mo | 6.220E-08 | -1.948E+01 | 3.970E+00 | -0.000001 |
| Ni | 1.749E-06 | -2.289E+00 | 9.915E-01 | -0.000004 |
| V | 7.407E-09 | -2.394E+01 | 1.514E+01 | 0.000000 |
| W | 1.800E-09 | -1.168E+02 | 6.528E+01 | 0.000000 |
| Sm | 1.092E-09 | -3.345E+03 | 4.425E+01 | -0.000004 |
| Dy | 8.640E-10 | -1.020E+03 | 7.432E+01 | -0.000001 |
| Eu | 9.239E-10 | -3.797E+03 | 1.058E+02 | -0.000004 |
| Gd | 8.929E-10 | -2.026E+04 | 9.861E+01 | -0.000018 |
| | | | Sum in Quadrature | 0.000076 |

Table 41. Results of the Analysis of the Fuel Impurities Uncertainty.

| Case | $\Delta k_{eff}$ | |
|---|---|---|
| | Value | Uncertainty |
| 1 | 0.000076 | 0.000003 |
| 2 | 0.000076 | 0.000003 |
| 3 | 0.000077 | 0.000003 |
| 4 | 0.000077 | 0.000003 |
| 5 | 0.000077 | 0.000003 |
| 6 | 0.000078 | 0.000003 |
| 7 | 0.000077 | 0.000003 |
| 8 | 0.000078 | 0.000003 |
| 9 | 0.000077 | 0.000003 |
| 10 | 0.000078 | 0.000003 |
| 11 | 0.000079 | 0.000003 |
| 12 | 0.000077 | 0.000002 |
| 13 | 0.000077 | 0.000002 |
| 14 | 0.000077 | 0.000002 |
| 15 | 0.000077 | 0.000002 |
| 16 | 0.000076 | 0.000002 |
| 17 | 0.000077 | 0.000002 |
| 18 | 0.000076 | 0.000002 |
| 19 | 0.000076 | 0.000002 |
| 20 | 0.000072 | 0.000002 |
| 21 | 0.000072 | 0.000002 |
| 22 | 0.000072 | 0.000002 |
| 23 | 0.000071 | 0.000001 |
| 24 | 0.000071 | 0.000001 |
| 25 | 0.000071 | 0.000001 |
| 26 | 0.000071 | 0.000002 |
| 27 | 0.000071 | 0.000001 |

# Example - Section 2 (LEU-COMP-THERM-102)

- Section 2.4 – Uncertainty Analyses

**2.4.13 Fuel Clad Composition** – The composition range for 3003 aluminum tubing is shown in Table 21. The composition limits are specified either as two bounding values giving minimum and maximum content of a given element or as a single bounding value giving the maximum allowed content of a given element. The assumption was made that any level of content between the limiting values is equally probable. Therefore, the probability distribution between the limits is constant. As a result, one standard deviation is the width of the interval divided by $\sqrt{3}$.

Under the assumption that the mass and volume of the cladding material are held constant and that changes in a constituent are counterbalanced by changes in the aluminum content, the sensitivity of the system $k_{eff}$ $S_C$ due to the uncertainty in any given constituent of the alloy can be obtained from

$$S_C = \frac{S_I}{N_I} - \frac{A_I S_{Al}}{M_{Al} N_{Al}}$$

where the symbols $S$, $N$, and $A$ indicate the same quantities as above; the subscript $I$ refers to the constituent species and the subscript $A_l$ refers to the aluminum in the cladding material. The uncertainty in $S_C$ is obtained by propagating the uncertainties in $S_I$ and $S_{Al}$ through the definition of $S_C$. Table 42 lists the uncertainty in the atom density of each fuel clad constituent, the sensitivity of the system $k_{eff}$ to the atom density uncertainties, and the $k_{eff}$ uncertainty that results from the uncertainty in each fuel clad constituent for Case 1. The $k_{eff}$ uncertainties for the individual constituents are summed in quadrature to obtain the overall contribution to the uncertainty in the system $k_{eff}$

# Example - Section 2 (LEU-COMP-THERM-102)

- Section 2.4 – Uncertainty Analyses

## 2.4.13 Fuel Clad Composition

Table 42. Atom Density Uncertainty and $k_{eff}$ Sensitivity for the Fuel Clad Impurities for Case 1.

| Impurity | Uncertainty ($b^{-1}$ $cm^{-1}$) | Sensitivity (b cm) | | $\Delta k_{eff}$ |
|---|---|---|---|---|
| | | Value | Unc. | |
| Si | 1.014E-04 | 3.027E-02 | 3.921E-02 | 0.000003 |
| Fe | 5.949E-05 | -7.865E-01 | 7.952E-02 | -0.000047 |
| Cu | 1.120E-05 | -1.320E+00 | 1.437E-01 | -0.000015 |
| Mn | 4.319E-05 | -3.938E+00 | 7.208E-02 | -0.000170 |
| Zn | 7.259E-06 | -4.518E-01 | 2.315E-01 | -0.000003 |
| | | | Sum in Quadrature | 0.000177 |

Table 43. Results of the Analysis of the Fuel Clad Constituents Uncertainty.

| Case | $\Delta k_{eff}$ | |
|---|---|---|
| | Value | Uncertainty |
| 1 | 0.000177 | 0.000007 |
| 2 | 0.000174 | 0.000007 |
| 3 | 0.000174 | 0.000007 |
| 4 | 0.000172 | 0.000007 |
| 5 | 0.000169 | 0.000008 |
| 6 | 0.000171 | 0.000007 |
| 7 | 0.000167 | 0.000007 |
| 8 | 0.000172 | 0.000006 |
| 9 | 0.000161 | 0.000006 |
| 10 | 0.000172 | 0.000006 |
| 11 | 0.000164 | 0.000006 |
| 12 | 0.000152 | 0.000005 |
| 13 | 0.000151 | 0.000005 |
| 14 | 0.000148 | 0.000005 |
| 15 | 0.000152 | 0.000004 |
| 16 | 0.000150 | 0.000004 |
| 17 | 0.000148 | 0.000005 |
| 18 | 0.000151 | 0.000004 |
| 19 | 0.000150 | 0.000004 |
| 20 | 0.000136 | 0.000003 |
| 21 | 0.000137 | 0.000004 |
| 22 | 0.000136 | 0.000003 |
| 23 | 0.000136 | 0.000003 |
| 24 | 0.000136 | 0.000003 |
| 25 | 0.000133 | 0.000003 |
| 26 | 0.000132 | 0.000003 |
| 27 | 0.000133 | 0.000003 |

# Example - Section 2 (LEU-COMP-THERM-102)

- Section 2.4 – Uncertainty Analyses

**2.4.2 Clad Outer Diameter –** The outer diameter of the fuel rod clad tubes was measured for the 2194 rods available for the experiments. The population average for the measurements was 0.249980 in (0.634948 cm as rounded from the original data) with a standard deviation of 0.000086 in (0.000218 cm). The uncertainty in the mean value is 0.0000047 in (0.0000085 cm), the standard deviation divided by the square root of 338, the lowest number of fuel rods in any of the benchmark experiment configurations. Because the outside diameter was known for each fuel rod and the identity of each fuel rod in every configuration was known, the distribution of the fuel rod diameters does not contribute to the uncertainty in the experiments. The systematic uncertainty in the measurements was 0.000022 in (0.000056 cm). The resolution of the instruments used was 0.000001 in (0.00000254 cm) and the repeatability was 0.000005 in (0.0000127 cm). The random uncertainty in the diameter measurements was 0.000030 in (0.0000762 cm) and will be treated as a systematic uncertainty. The sum in quadrature of the systematic uncertainties (0.000022 in, 0.000001 in, 0.000005 in, and 0.000030 in) is 0.0000375 in (0.0000954 cm). Arrays with fuel rod clad diameters up to 0.00508 cm on either side of the nominal value were analyzed to determine the sensitivity of the experiments to the clad tube diameter. The mass of the clad tube was kept constant during these variations. The results of the analysis of the clad outer diameter uncertainty are shown in Table 30.

# Example - Section 2 (LEU-COMP-THERM-102)

- Section 2.4 – Uncertainty Analyses

**2.4.2 Clad Outer Diameter**

Table 30. Results of the Analysis of the Clad Outer Diameter Uncertainty.

| Case | Uncertainty Value (cm) | Sensitivity ($cm^{-1}$) | | $\Delta k_{eff}$ | |
|---|---|---|---|---|---|
| | | Value | Uncertainty | Value | Uncertainty |
| 1 | 0.0000954 | -1.2209 | 0.0070 | -0.000116 | 0.000001 |
| 2 | 0.0000954 | -1.2390 | 0.0070 | -0.000118 | 0.000001 |
| 3 | 0.0000954 | -1.2189 | 0.0070 | -0.000116 | 0.000001 |
| 4 | 0.0000954 | -1.1791 | 0.0070 | -0.000112 | 0.000001 |
| 5 | 0.0000954 | -1.1354 | 0.0070 | -0.000108 | 0.000001 |
| 6 | 0.0000954 | -1.0886 | 0.0070 | -0.000104 | 0.000001 |
| 7 | 0.0000954 | -0.9965 | 0.0070 | -0.000095 | 0.000001 |
| 8 | 0.0000954 | -0.9961 | 0.0070 | -0.000095 | 0.000001 |
| 9 | 0.0000954 | -0.9843 | 0.0070 | -0.000094 | 0.000001 |
| 10 | 0.0000954 | -0.9437 | 0.0070 | -0.000090 | 0.000001 |
| 11 | 0.0000954 | -0.9008 | 0.0070 | -0.000086 | 0.000001 |
| 12 | 0.0000954 | -0.4142 | 0.0070 | -0.000040 | 0.000001 |
| 13 | 0.0000954 | -0.4138 | 0.0070 | -0.000039 | 0.000001 |
| 14 | 0.0000954 | -0.4000 | 0.0070 | -0.000038 | 0.000001 |
| 15 | 0.0000954 | -0.3858 | 0.0070 | -0.000037 | 0.000001 |
| 16 | 0.0000954 | -0.3350 | 0.0070 | -0.000032 | 0.000001 |
| 17 | 0.0000954 | -0.3343 | 0.0070 | -0.000032 | 0.000001 |
| 18 | 0.0000954 | -0.3213 | 0.0070 | -0.000031 | 0.000001 |
| 19 | 0.0000954 | -0.2957 | 0.0070 | -0.000028 | 0.000001 |
| 20 | 0.0000954 | -0.0933 | 0.0056 | -0.000009 | 0.000001 |
| 21 | 0.0000954 | -0.0992 | 0.0063 | -0.000009 | 0.000001 |
| 22 | 0.0000954 | -0.0945 | 0.0056 | -0.000009 | 0.000001 |
| 23 | 0.0000954 | -0.0705 | 0.0056 | -0.000007 | 0.000001 |
| 24 | 0.0000954 | -0.0520 | 0.0056 | -0.000005 | 0.000001 |
| 25 | 0.0000954 | -0.0555 | 0.0056 | -0.000005 | 0.000001 |
| 26 | 0.0000954 | -0.0354 | 0.0056 | -0.000003 | 0.000001 |
| 27 | 0.0000954 | -0.0350 | 0.0056 | -0.000003 | 0.000001 |

# Example - Section 2 (LEU-COMP-THERM-102)

- Section 2.4 – Uncertainty Analyses

**2.4.16 Temperature –** The experiments were run near a temperature of 25 °C and the data were corrected to that temperature. A bounding estimate of the uncertainty in the experiment temperature is 1 °C, which is based on the calibration and performance characteristics of type K thermocouples used. The sensitivity of the arrays to the fuel and moderator/reflector temperature was determined by analyzing arrays at temperatures from 5 °C to 50 °C in 5 °C increments using MCNP6.1.1 and ENDF/B-VII.1 cross sections. In the analysis, the water temperature was varied as well as the water density. Thermal scattering kernel data appropriate for each water temperature were used during the variations. The sensitivity of the arrays to fuel temperature was also computed with the same code/cross sections using the temperature-dependent uranium cross sections included with the code. Thermal expansion of the $UO_2$ was included in the analysis. The variations in the calculated $k_{eff}$ data in both cases necessitated the use of a second-order polynomial fit. The sensitivity was taken as the slope of the polynomial at the experiment temperature. The stochastic uncertainties in the Monte Carlo calculations were propagated through the fit. The two sensitivities were combined to obtain the overall temperature sensitivity of the assemblies. The uncertainties in the two sensitivities were combined in quadrature.

- Uncertainty in experiment temperature estimated to be 1°C (based on thermocouples used)
- MCNP calculations with water temperature and density varied (5°C to 50°C in 5°C increments)
- Fuel thermal expansion and Doppler broadening of the cross-section resonances included
- Appropriate thermal scattering kernel data for each water temperature used
- Second-order polynomial fit to the data – slope gives sensitivity

# Example - Section 2 (LEU-COMP-THERM-102)

- Section 2.4 – Uncertainty Analyses

**2.4.16 Temperature**

Moderator, reflector, and fuel temperature

Temperature (includes density, thermal expansion, and appropriate nuclear data sets)

Table 48. Results of the Analysis of the Temperature Uncertainty.

| Case | Uncertainty Value (°C) | Sensitivity (°C$^{-1}$) | | $\Delta k_{eff}$ | |
|---|---|---|---|---|---|
| | | Value | Uncertainty | Value | Uncertainty |
| 1 | 1 | -0.0000155 | 0.0000008 | -0.000016 | 0.000001 |
| 2 | 1 | -0.0000155 | 0.0000008 | -0.000015 | 0.000001 |
| 3 | 1 | -0.0000150 | 0.0000008 | -0.000015 | 0.000001 |
| 4 | 1 | -0.0000152 | 0.0000008 | -0.000015 | 0.000001 |
| 5 | 1 | -0.0000128 | 0.0000008 | -0.000013 | 0.000001 |
| 6 | 1 | -0.0000118 | 0.0000008 | -0.000012 | 0.000001 |
| 7 | 1 | -0.0000156 | 0.0000008 | -0.000016 | 0.000001 |
| 8 | 1 | -0.0000154 | 0.0000008 | -0.000015 | 0.000001 |
| 9 | 1 | -0.0000160 | 0.0000008 | -0.000016 | 0.000001 |
| 10 | 1 | -0.0000148 | 0.0000008 | -0.000015 | 0.000001 |
| 11 | 1 | -0.0000115 | 0.0000008 | -0.000012 | 0.000001 |
| 12 | 1 | -0.0000253 | 0.0000008 | -0.000025 | 0.000001 |
| 13 | 1 | -0.0000243 | 0.0000008 | -0.000024 | 0.000001 |
| 14 | 1 | -0.0000209 | 0.0000008 | -0.000021 | 0.000001 |
| 15 | 1 | -0.0000174 | 0.0000008 | -0.000017 | 0.000001 |
| 16 | 1 | -0.0000234 | 0.0000008 | -0.000023 | 0.000001 |
| 17 | 1 | -0.0000235 | 0.0000008 | -0.000023 | 0.000001 |
| 18 | 1 | -0.0000180 | 0.0000008 | -0.000018 | 0.000001 |
| 19 | 1 | -0.0000131 | 0.0000008 | -0.000013 | 0.000001 |
| 20 | 1 | 0.0000114 | 0.0000008 | 0.000011 | 0.000001 |
| 21 | 1 | 0.0000130 | 0.0000008 | 0.000013 | 0.000001 |
| 22 | 1 | 0.0000222 | 0.0000008 | 0.000022 | 0.000001 |
| 23 | 1 | 0.0000297 | 0.0000008 | 0.000030 | 0.000001 |
| 24 | 1 | 0.0000298 | 0.0000008 | 0.000030 | 0.000001 |
| 25 | 1 | 0.0000321 | 0.0000008 | 0.000032 | 0.000001 |
| 26 | 1 | 0.0000428 | 0.0000008 | 0.000043 | 0.000001 |
| 27 | 1 | 0.0000522 | 0.0000008 | 0.000052 | 0.000001 |

# Section 2 (LEU-COMP-THERM-102)

- Section 2.4 – Uncertainty Analyses

**2.4.17 Uncertainty Values –** The effects of several uncertainty components in the critical experiments on the k $_{eff}$ of the configurations are analyzed above. The total uncertainty for each case was obtained by combining in quadrature the case-wise results. The total uncertainty so obtained for each case is listed in Table 49. These values represent the uncertainty in the experiments at the one-standard-deviation level.

| Case | $\Delta k_{eff}$ |
|---|---|
| 1 | 0.00106 |
| 2 | 0.00106 |
| 3 | 0.00107 |
| 4 | 0.00105 |
| 5 | 0.00104 |
| 6 | 0.00100 |
| 7 | 0.00096 |
| 8 | 0.00095 |
| 9 | 0.00093 |
| 10 | 0.00094 |
| 11 | 0.00090 |
| 12 | 0.00067 |
| 13 | 0.00067 |
| 14 | 0.00065 |
| 15 | 0.00063 |
| 16 | 0.00063 |
| 17 | 0.00062 |
| 18 | 0.00062 |
| 19 | 0.00062 |
| 20 | 0.00093 |
| 21 | 0.00095 |
| 22 | 0.00099 |
| 23 | 0.00104 |
| 24 | 0.00110 |
| 25 | 0.00111 |
| 26 | 0.00115 |
| 27 | 0.00120 |

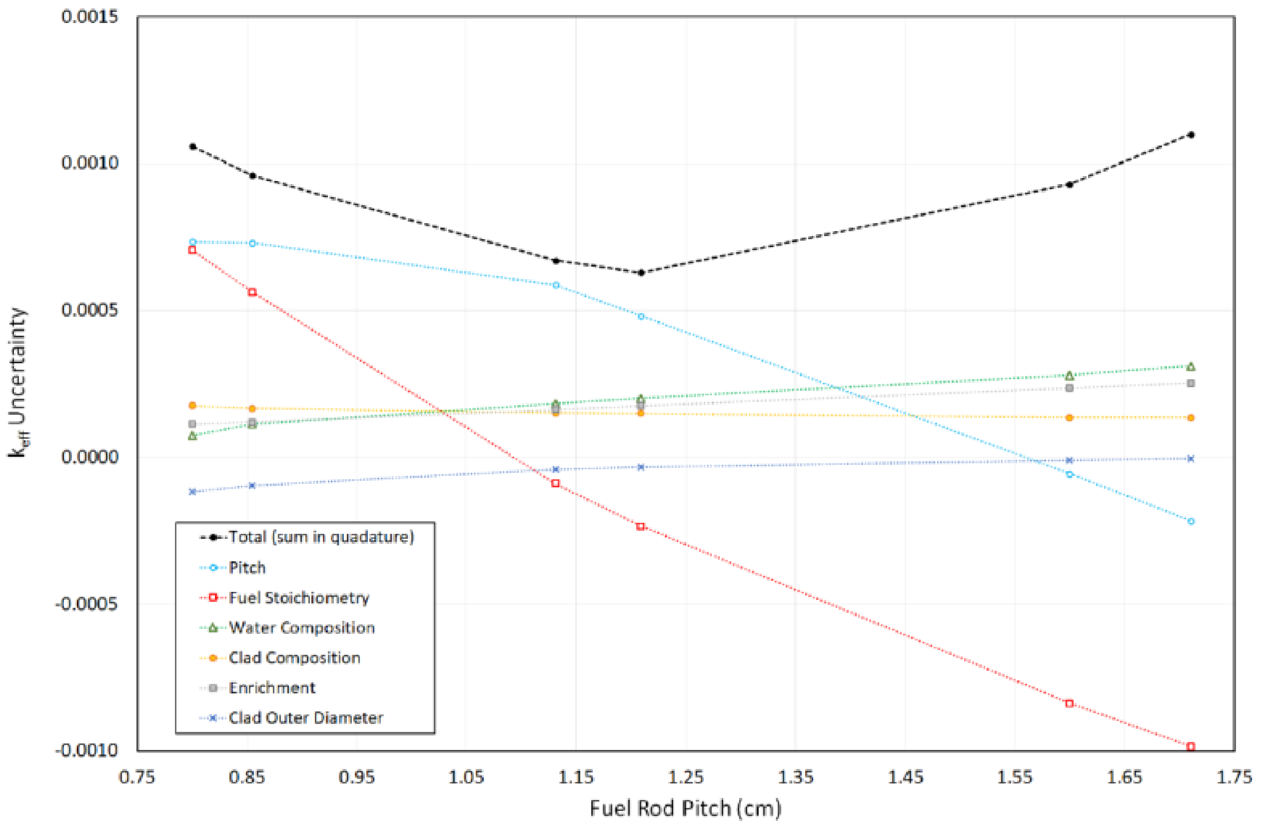


Figure 50. Calculated $k_{eff}$ Uncertainty as a Function of Fuel Rod Pitch.

# Section 2 – Common Mistakes/Gotchas

- Not defining ‘negligible’ (the meaning of ‘negligible’ needs to be quantified)
  - The effect of an uncertainty may be evaluated simply as ‘negligible’
- Discussing the model
  - Sometimes the lines are blurred between the benchmark experiment, experiment uncertainty, the benchmark model, and model bias
- Significant figures
  - Attention in all sections
- Proved complete source information
  - Attention in all sections
- Inconsistencies in values rounded from original data
  - Minor issue, but needs to be noted where applicable
- Resist tendency to overestimate uncertainty
  - It is a misconception that making large uncertainty estimates is always a conservative approach
- Not consulting with experts or seeking out pertinent literature
  - Uncertainty should be based on an understanding of the physical phenomena

# Acknowledgements

NUCLEAR CRITICALITY SAFETY PROGRAM
U.S. DEPARTMENT OF ENERGY


- The critical experiments at Sandia are supported by the DOE Nuclear Criticality Safety Program (NCSP), funded and managed by the National Nuclear Security Administration for the Department of Energy.